

PCI

Preclinical MRI of Neurological Diseases - Cellular and Molecular Imaging

Jan Klohs and Sarah Herrmann

Innovation with Integrity

Introduction

Major neurological disorders like Alzheimer's disease, Parkinson's disease, epilepsy, multiple sclerosis, stroke, and brain tumors are leading causes of disability and death globally. They pose a massive clinical, social, and economic burden. Intensive research efforts have revealed a complex interplay between the molecular and cellular components of the nervous tissue, the cerebral vasculature, and the immune system that are involved in the genesis, progression, and maintenance of central nervous system (CNS) disorders. The dynamic nature of these processes and their interactions necessitates system approaches to study them in the intact organism. Investigations are often conducted in laboratory mice and rats, given their genetic and biological similarities to humans and the large availability of neurological disease conditions that can either be induced by experimental manipulations, genetic engineering, or by altering diets and environmental conditions. Moreover, novel therapeutic approaches such as immuno-, gene and cell therapy, brain machine interfaces, and precise drug delivery techniques that are developed to mitigate or cure neurological diseases, for which often only few effective therapies exist, require thorough preclinical evaluation in animal models before translation to patients. Therefore, methods that non-invasively visualize cellular and molecular processes of the CNS in small animals are highly desired.

Bruker offers a portfolio of preclinical imaging instruments comprising modalities such as magnetic resonance imaging (MRI), position emission tomography (PET), and single photon emission computed tomography (SPECT) that are well suited for cellular and molecular imaging applications. Among them, MRI has found extensive implementations in assessing CNS pathology, providing information about changes in the anatomy, organization, and circuitry of the brain and spinal cord, and yielding quantitative MRI measures of microstructure and tissue composition as well as of metabolic and functional processes. Bruker's innovative MRI instrument design encompasses BioSpec Maxwell instruments starting at 3 Tesla, classic MRIs, and ultra-high field MRIs culminating with the BioSpec 18 Tesla. Instruments are equipped with state-of-the-art hardware components from high performance gradients to the electronic architecture to radiofrequency coils, dedicated for imaging the brain and spinal cord of mice and rats and other model organisms, that together facilitate data acquisition with high speed and quality, covering a wide range of applications. Bruker's ParaVision software comes with protocols that are pre-optimized for small rodent species and corresponding applications. It contains advanced imaging viewing, reconstruction, and analysis options, as well as a software framework for individual MR method development.

Recent progress in chemistry, molecular and cell biology, and nanotechnology has expanded the strength of MRI to characterize pathological tissue changes by providing tools that visualize cellular and molecular processes. A wealth of novel imaging probes, reporter gene - and cell labelling strategies provide the basis for gaining unprecedented insight into the pathomechanisms of neurological disorders. Here, we illustrate examples from academic research groups' work on the application of molecular and cellular MRI in models of neurological disorders and its use for evaluation of gene and cell therapies.

Mapping Molecular Processes and Gene Expression

Targeted MRI probes are designed and synthesized for the visualization of specific pathophysiological molecular processes. MRI probes are commonly made of contrast agents such as iron oxide nanoparticles, paramagnetic compounds (e.g., Gadolinium), chemical exchange saturation transfer (CEST)- and paramagnetic CEST (PARACEST)- agents, or perfluorocarbons (^{19}F) and a targeting moiety such as an antibody, peptide, oligonucleotide, enzyme substrate, etc. (Fig. 1). For example, microsized matrix-based magnetic particles (M3P) were used for the detection of brain inflammation.¹ M3P were synthesized by a self-assembly of catechol-coated magnetite nanocrystals (Fig. 2A). The M3P have a high payload of superparamagnetic material and display biocompatibility and water dispersibility. M3P were conjugated to antibodies against the vascular cell adhesion molecule 1 (VCAM-1) as an indicator of endothelial activation. T2*-weighted MRI showed local accumulation of VCAM-1-targeted M3P in the striatum after lipopolysaccharide injection, that induced focal neuroinflammation. M3P was also used to detect the inflammatory response to focal cerebral ischemia in the mouse brain.

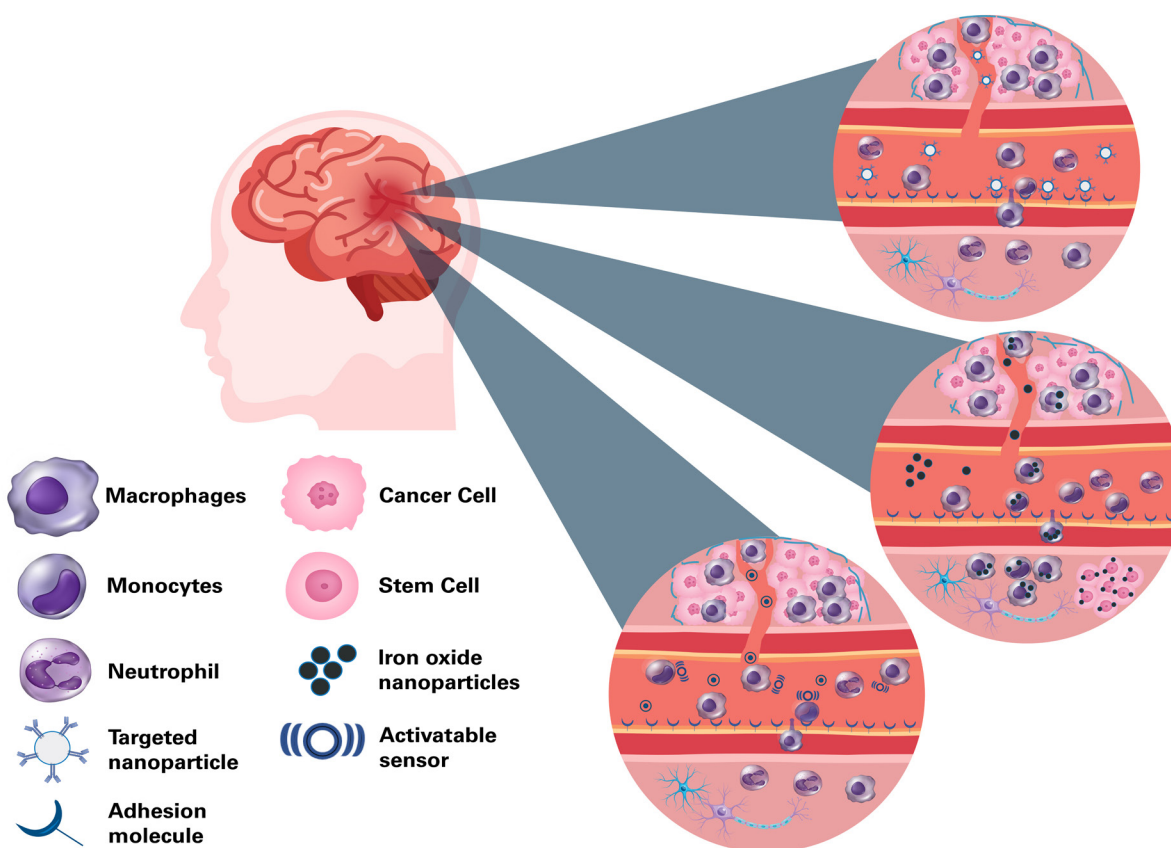


Figure 1 Approaches for cellular and molecular imaging of brain tumors. **Top:** Targeted MRI probes bind to receptors that are highly expressed in tumors, for example vascular adhesion molecules. **Middle:** Cell labeling and reporter genes can track the dynamics of immune cell trafficking and the fate of cell-based therapies. Cells can either be labeled with an MRI contrast agent, often an iron oxide nanoparticle, or be transfected with a plasmid containing a reporter gene. The gene product in the cells gives rise to a detectable MRI contrast. Labeled cells are either transplanted locally (e.g. stem cells) or are injected systemically (e.g. monocytes), where they migrate to their target site. Alternatively, nanoparticles are injected intravascularly where they are taken up by phagocytosing cells like macrophages. **Bottom:** Injected activatable sensors report enzyme activity, thus providing highly specific molecular markers of the tumor pathology.

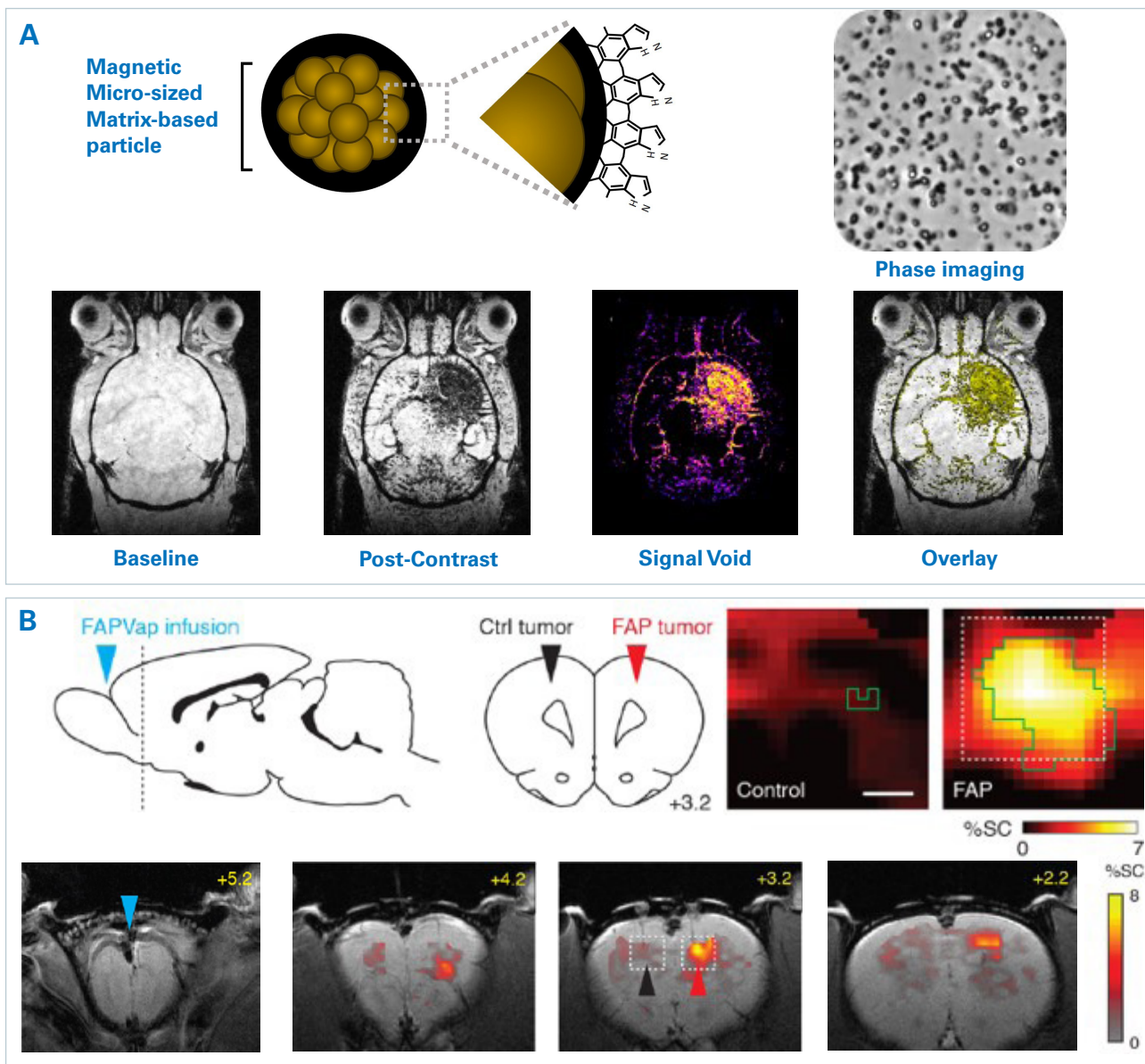


Figure 2 Examples of molecular MRI. A) Immuno-MRI with micro-sized matrix-based particles (M3P). **Top:** Representation of the structure and surface of MP3 and phase contrast microscopy. **Bottom:** T2*-weighted images of a mouse brain are depicted at baseline and 10 minutes after injection of M3P conjugated with monoclonal antibodies against VCAM-1. The mouse had been injected with lipopolysaccharide into the right striatum 24h prior MRI. The resulting signal void and overlay are also shown. Images were taken from Martinez de Lizarrondo et al. 2022,¹ with modifications. The work has been published under a Creative Commons Attribution License 4.0 (<https://creativecommons.org/licenses/by/4.0/>) **B)** Hemodynamic molecular MRI of tumor-associated enzyme activity. **Top left:** An FAP-activatable probe was infused into the subarachnoid space caudal to the olfactory bulb and rostral to the tumors (blue arrowhead). FAP-expressing (red arrowhead) and control (black arrowhead) tumors were inoculated into the dorsal cortex (dashed line) in rats. **Bottom:** T2*-weighted MRI reveal signal change (color) following FAP-sensitive vasoprobe infusion in the presence of control (black arrowhead) and FAP-expressing (red arrowhead) xenografts overlaid on an anatomical image. Scale bar = 4 mm. **Top right:** Zoom-ins on tumor regions (dotted boxes). Scale bar = 0.5 mm. Images were taken from Desai et al. 2021,² with modifications. The work has been published under a Creative Commons Attribution License 4.0 (<https://creativecommons.org/licenses/by/4.0/>).

In a different approach, an activatable probe was designed and used for the detection of fibroblast activation protein (FAP) activity in brain tumors.² FAP is highly expressed by many types of tumors, including glioblastomas. Sensors are derived from peptides fused to an FAP-labile blocking domain. When the FAP uncages the peptide, it induces a vasodilation which in turn can be detected by MRI. The feasibility of detecting FAP-expressing tumors *in vivo* was shown (Fig. 2B). FAP-expressing and control tumors were inoculated into the dorsal cortex in rats. The FAP-activatable probe was infused into the subarachnoid space caudal to the olfactory bulb and rostral to the tumors. T2*-weighted MRI revealed activation of the probe at the FAP-expressing tumor, demonstrating the specificity of the approach.

Reporter gene assays are developed for studying expression of specific genes (e.g. oncogenes, cytokine- or chemokine-related genes). Reporter genes are transfected into cells or are delivered by viral vectors to specific tissues (**Fig. 1**). The gene of interest and the reporter protein are driven by the same promoter. When both genes are expressed, the produced reporter proteins give rise to a detectable MRI contrast. Common MRI reporters are iron chelating and storing proteins or enzymes (e.g., tyrosinase, ferritin) that increase the intracellular concentration of paramagnetic iron, thereby reducing relaxation rates and producing contrast in T1- and T2-weighted MR images.³ Alternative approaches aim to increase intracellular protein concentration or change water diffusivity of cells.^{4,5}

As a reporter MRI approach, a lysine-rich protein (LRP) reporter gene has been developed.⁴ The LRP reported was expressed in glioma cells that were inoculated into mice brains (**Fig. 3A**). Glioma cells transfected with an empty construct served as control. CEST-MR images were acquired before and after oncolytic herpes simplex virus (oHSV) therapy. A significant increase in the tumor amide-CEST contrast was obtained for LRP-expressing tumors compared to control that was aggravated by the oHSV treatment.

An alternative method employed aquaporin 1 (AQP1) as a new genetically encoded reporter.⁵ The expression of AQP1 leads to a change in tissue water diffusivity that can be detected by diffusion weighted MRI (**Fig. 3B**). Tumor cells expressing either AQP1 or green fluorescent protein as controls were inoculated into the right and left striatum of a mouse. Reporter gene expression was controlled by doxycycline administration. Diffusion MRI showed a marked signal decrease in the AQP1 tumor after doxycycline treatment.

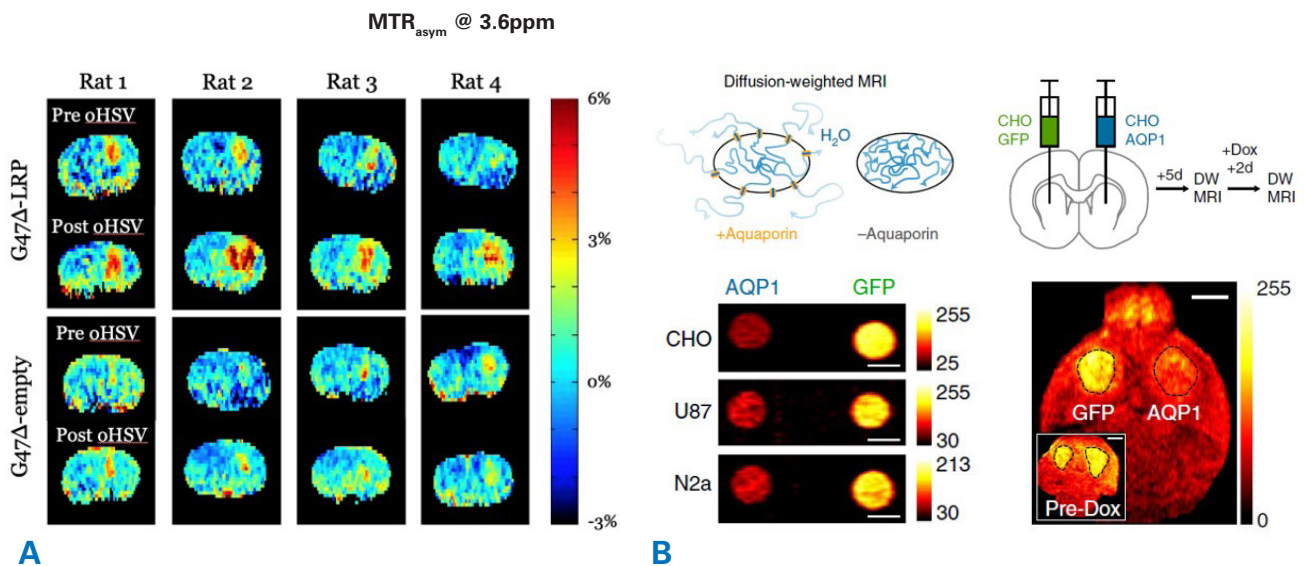


Figure 3 Examples molecular MRI using reporter gene approaches. **A)** CEST-MRI imaging of oncolytic virus therapy in brain tumors using LRP reporter. Shown are amide proton CEST amplitude maps of eight rats before and after oncolytic herpes simplex virus (oHSV) therapy. Animals were inoculated with tumor cells that were transfected to express either LRP ($G_{47\Delta}$ -LRP) or received a control construct ($G_{47\Delta}$ -empty). The oncolytic virus therapy leads to an increased LRP signal within the tumors. Courtesy: Christian T. Farrar, Department of Radiology, Athinoula A. Martinos Center for Biomedical Imaging, Massachusetts General Hospital and Harvard Medical School, USA. **B)** Aquaporin 1 (AQP1) as a new genetically encoded reporter for diffusion weighted MRI. **Top:** Illustration showing the change in water diffusion when a cell expresses aquaporin receptors. **Bottom left:** Diffusion-weighted images of CHO, U87, and Neuro 2a cell expressing either AQP1 or green fluorescent protein. Scale bars = 3 mm. **Bottom right:** Tumor cells expressing either AQP1 or green fluorescent protein under the CHO promoter were inoculated into the right and left striatum of a mouse. Diffusion-weighted MRI was performed before and after doxycycline (Dox) administration. Representative diffusion-weighted image of a coronal brain slice with bilateral tumor xenografts, 48 h after doxycycline administration. Inset shows a diffusion-weighted image of the same mouse acquired before doxycycline injection. Scale bar = 2 mm. Images were taken from Mukherjee et al. 2016,⁵ with modifications. The work has been published under a Creative Commons Attribution License 4.0 (<https://creativecommons.org/licenses/by/4.0/>).

Monitoring of Cell Trafficking and Cell Therapies

MRI can be used to track the fate of cell populations that are involved in the development of neurological disorders (e.g. tumor, immune cells) or repair (e.g. neuronal stem cells, oligodendrocyte precursors, or macrophages). Cells are either labeled by contrast agents (iron oxide nanoparticles, ^{19}F compounds, etc.) or reporter genes (Fig. 1). The use of reporter gene approaches offers the advantage that they do not only label the cells but may also report on the functional states of the cells when a specific gene is expressed. Cells can be labelled or are transfected *in vitro* and are then implanted or injected into the animal. Alternatively, contrast agents can be injected systemically, where they are taken up by phagocytotic cells. An inherent challenge is the presence of the blood-brain or blood-spinal cord barriers that may hinder the delivery of systemically administered cells to their target within the CNS. Thus, cell delivery can be combined with approaches to disrupt or circumvent such barriers such as MRI-guided focused ultrasound.

In MRI cell tracking, signal is usually detected from bulk cells within tissue, but single cell tracking in the mouse brain in real time has been demonstrated.⁶ T2*-weighted images of a naïve mouse acquired with twenty timeframes (from 8 until 164 min) after intravenous injection of iron oxide nanoparticles show hypointense spots, representing mononuclear phagocytes that have taken up the injected nanoparticles (Fig. 4A). Furthermore, time-lapse MRI was applied to mice with experimental autoimmune encephalomyelitis (EAE) and control mice after injection of monocytes exogenously labelled with iron oxide nanoparticles. Labeled monocytes migrate to the inflammatory lesion in the brain and the lesion in EAE mice. The number of counted hypointense spots were significantly higher in naïve as compared to EAE mice, both at the pre-symptomatic and symptomatic stage, reflecting adhesion of patrolling monocytes to the vasculature at the sites of inflammation in EAE mice.

A

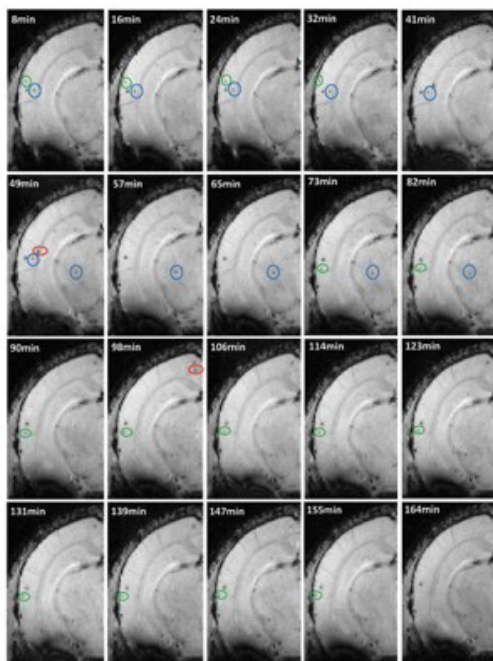
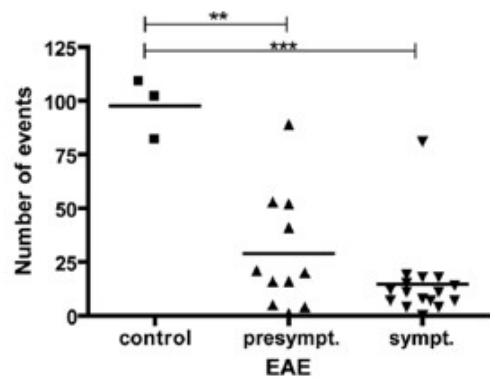
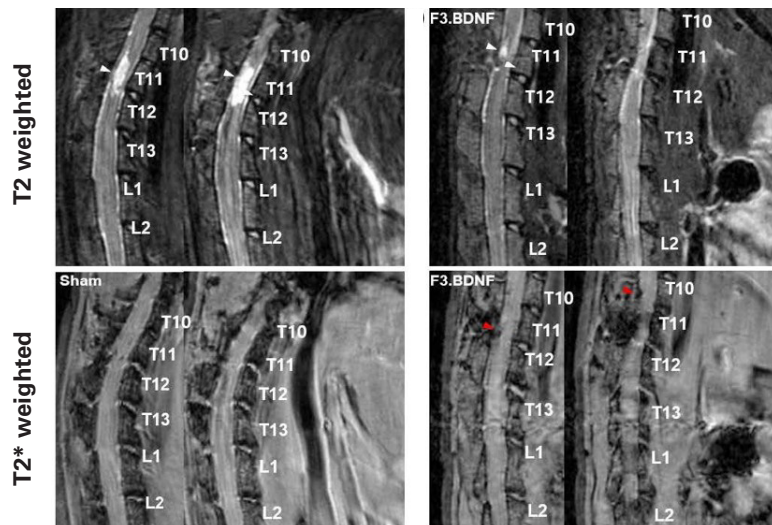


Figure 4 Examples for using MRI for examining cell therapy. A) Top: Time-lapse MRI for tracking inflammatory cells. Shown are 20 time frames (8, 16,...until 164 min) of one coronal T2*-weighted image from a brain of naïve mouse after intravenous injection of iron oxide nanoparticles. Hypointense spots represent labelled immune cells. **Bottom:** Cell trafficking was assessed in EAE and control mice after injection of iron oxide nanoparticle labelled monocytes. The number of counted hypointense spots (overall events) were significantly higher in naïve as compared to EAE mice, both at the pre-symptomatic and symptomatic stage. ** $p < 0.01$ and *** $p < 0.001$. Images were taken from Masthoff et al. 2018,⁶ with modifications. The work has been published under a Creative Commons Attribution License 4.0 (<https://creativecommons.org/licenses/by/4.0/>). **B)** Detection of Feridex®-labeled human neural stem cells overexpressing brain-derived neurotrophic factor (F3.BDNF) in a rat contusion model of spinal cord injury. T2-weighted and T2*-weighted MRI images at 72 days after contusive spinal cord injury and infusion of either F3.BDNF cells or medium as control. The white arrowheads indicate the lesion, while the red arrowheads indicate labeled F3.BDNF cells. There is a marked reduction in the hyperintense lesion between the F3.BDNF group and control. Images were taken from Chang et al. 2021,⁷ with modifications. The work has been published under a Creative Commons Attribution License 4.0 (<https://creativecommons.org/licenses/by/4.0/>).

B



MRI can also be used to track the fate of cell and tissue transplants aimed to replace and repair damaged cells and/or tissue and to augment endogenous restorative mechanisms aiming to repair or regenerate damaged nervous tissue. It allows to follow the trafficking of cells to the target site and assessment of engraftment and long-term viability. For example, transplantation of human neural stem cells overexpressing brain-derived neurotrophic factor (F3.BDNF) in a rat spinal cord was explored as a therapy for a contusion injury.⁷ F3.BDNF cells were labeled with Feridex® prior transplantation. T2-weighted imaging was used to demark the development of the lesion, while T2*-weighted imaging was used for the detection of transplanted F3.BDNF cells (**Fig. 4B**). Labeled F3.BDNF cells were found to traffic to the lesion site, concomitant with a marked reduction in the hyperintense lesion compared to control. Furthermore, immunohistochemistry showed that the transplanted F3.BDNF differentiated into neurons, oligodendrocytes, and astrocytes in the injured spinal cord. Cell transplantation resulted in reduced inflammatory response at the lesion site and led to improved functional recovery in the injured rats.

MRI and magnetic resonance spectroscopy (MRS) are also indispensable tools to assess the behavior of incorporated cells and tissue graft in the host tissue and the functional tissue changes that result from therapy such as to assess gross structural changes (e.g. reduction in lesion extent), tissue remodeling (e.g. remyelination, angiogenesis, changes in connectivity) and functional tissue changes (e.g. neuroplasticity, neurotransmitter concentration).

Theranostics and Evaluation of Gene Therapies

MRI probes can be designed as theranostics when they contain therapeutic agents in addition to a signal moiety. MRI can be used to monitor the delivery and/or release of the therapeutic agents at the target site. For example, ¹⁹F MRI was used to image Siponimod, a drug used in multiple sclerosis to reduce the infiltration of inflammatory lymphocytes into the CNS.⁸ After oral administration in mice, the drug was detected with ¹⁹F MRI *in vivo* in the stomach and over time also in the liver, demonstrating the absorption of the drug from the stomach (**Fig. 5A**). *Ex vivo* 3D ultra-short echo-time (UTE) MR images of the brain demonstrated that the drug passes over the blood-brain barrier and accumulates in brain regions with different concentrations.

To ameliorate neurological diseases related to missing or defective genes, and to treat brain tumors and acquired brain and spinal cord injuries, gene therapy aims to deliver functional genetic material to cells in the CNS. Defective genes can be corrected by introducing a functional copy of the gene, by silencing a mutant allele using ribonucleic acid (RNA) interference, by introducing a disease-modifying gene, or by using gene-editing technology (e.g. CRISPR/Cas). MRI can be helpful to guide the focal administration of gene material. Once a copy of a therapeutic gene is delivered to affected cells in the CNS, the product encoded by that gene (i.e., its messenger RNA and/or proteins) will be synthesized within the cells, utilizing the cells transcriptional and translational machinery, offering a potentially life-long therapeutic effect. Once delivered, the stably expressed transgene(s) can be visualized with MRI using reporter gene strategies or probes. Importantly, MRI and MRS can be used to probe tissue characteristics and thus to provide an early assessment of therapeutic efficiency as well as to longitudinally monitor effects of therapy. For example, serial MRI and MRS were used to monitor therapy of adeno-associated virus-mediated gene delivery in a mouse model of Canavan disease.⁹ In aspartoacylase (ASPA)-deficient lacZ-knock-in (AKO) mice ASPA deficiency leads to a build-up of N-acetyl-L-aspartate (NAA) and consequently to leukodystrophy. Serial T2-weighted MR imaging revealed progressive hyperintensities in the thalamus in AKO mice, resulting from spongiform vacuolization during disease progression. (**Fig. 5B**). Adeno-associated virus-mediated gene delivery in AKO mice at 22 weeks of age reduced brain NAA levels and ameliorated thalamic hyperintensities 4 weeks after injection. Other brain metabolites were found to normalize to control levels in response to the gene therapy 9 weeks after therapy. Gene therapy alleviated also astrogliosis, demyelination, and locomotor impairment seen in untreated AKO mice.

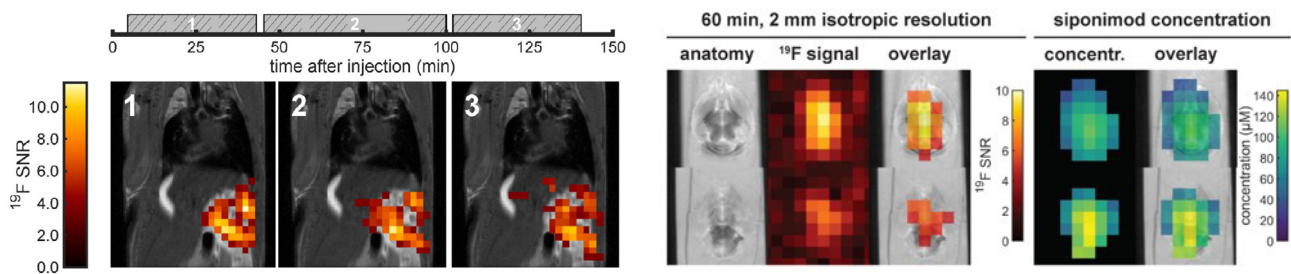
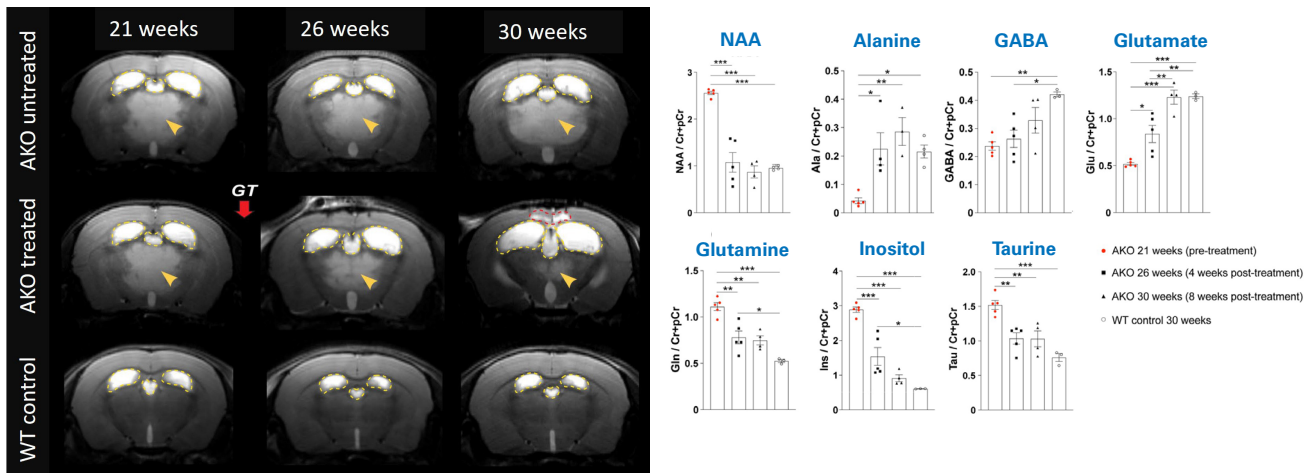
A**B**

Figure 5 Examples for using MRI for examining theranostic and gene therapy. **A)** Theranostic MRI of the multiple sclerosis drug Siponimod. **Left:** 2D ^{19}F UTE images overlaid on anatomical ^1H images. Each image corresponds to the average of 3×10 min ^{19}F acquisition acquired at different time intervals after oral administration of Siponimod (gray boxes). **Middle and right:** 3D UTE ^{19}F MRI in *ex vivo* brain tissue and Siponimod concentration estimates. Images were taken from Starke et al. 2023,⁸ with modification. The work has been published under a Creative Commons Attribution License 4.0 (<https://creativecommons.org/licenses/by/4.0/>). **B)** MRI therapy monitoring of adeno-associated virus-mediated gene delivery to a Canavan disease mouse model. Aspartoacylase (ASPA)-deficient lacZ-knock-in (AKO) mice replicate Canavan disease-like pathology. **Left:** Serial T2-weighted MR imaging revealed hyperintensities in the thalamus in AKO mice (yellow arrowheads) resulting from spongiform vacuolization. Yellow dashed lines outline the lateral and third ventricles. Adeno-associated virus-mediated gene therapy in AKO mice (AKO treated) at 22 weeks of age resulted in reduced vacuolization. **Right:** Serial MRS was used to assess changes in brain metabolites in response to the gene therapy. Gene therapy reduced NAA levels in AKO mice and normalized metabolite levels at 30 weeks of age. Images were taken from Fröhlich et al. 2022,⁹ with modifications. The work has been published under a Creative Commons Attribution License 4.0 (<https://creativecommons.org/licenses/by/4.0/>).

Conclusion

With the use of dedicated MRI imaging probes, cell labeling and reporter gene strategies, MRI has evolved from a modality that can report structural, functional, and metabolic tissue changes to a tool that can directly report cellular and molecular pathophysiological processes in the intact animal. Cellular and molecular MRI has been particularly useful for the characterization of the tumor microenvironment and in the evaluation of novel immune-, gene, and cell therapies for the treatment of neurological diseases by providing direct read-outs of therapy delivery and tissue response.

References:

1. Martinez de Lizarrondo S, Jacqmarcq C, Naveau M, Navarro-Oviedo M, Pedron S, Adam A, Freis B, Allouche S, Goux D, Razafindrakoto S, Gazeau F, Mertz D, Vivien D, Bonnard T, Gauberti M. Tracking the immune response by MRI using biodegradable and ultrasensitive microprobes. *Sci Adv*. 2022 Jul 15;8(28):eabm3596. doi: [10.1126/sciadv.abm3596](https://doi.org/10.1126/sciadv.abm3596).
2. Desai M, Sharma J, Slusarczyk AL, Chapin AA, Ohlendorf R, Wisniowska A, Sur M, Jasanoff A. Hemodynamic molecular imaging of tumor-associated enzyme activity in the living brain. *Elife*. 2021 Dec 21;10:e70237. doi: [10.7554/eLife.70237](https://doi.org/10.7554/eLife.70237).
3. Cai A, Zheng N, Thompson GJ, Wu Y, Nie B, Lin K, Su P, Wu J, Manyande A, Zhu L, Wang J, Xu F. Longitudinal neural connection detection using a ferritin-encoding adeno-associated virus vector and in vivo MRI method. *Hum Brain Mapp*. 2021 Oct 15;42(15):5010-5022. doi: [10.1002/hbm.25596](https://doi.org/10.1002/hbm.25596).
4. Perlman O, Ito H, Gilad AA, McMahon MT, ChioCCA EA, Nakashima H, Farrar CT. Redesigning reporter gene for improved proton exchange-based molecular MRI contrast. *Sci Rep*. 2020 Nov 26;10(1):20664. doi: [10.1038/s41598-020-77576-z](https://doi.org/10.1038/s41598-020-77576-z).
5. Mukherjee A, Wu D, Davis HC, Shapiro MG. Non-invasive imaging using reporter genes altering cellular water permeability. *Nat Commun*. 2016 Dec 23;7:13891. doi: [10.1038/ncomms13891](https://doi.org/10.1038/ncomms13891).
6. Masthoff M, Gran S, Zhang X, Wachsmuth L, Bietenbeck M, Helfen A, Heindel W, Sorokin L, Roth J, Eisenblätter M, Wildgruber M, Faber C. Temporal window for detection of inflammatory disease using dynamic cell tracking with time-lapse MRI. *Sci Rep*. 2018 Jun 22;8(1):9563. doi: [10.1038/s41598-018-27879-z](https://doi.org/10.1038/s41598-018-27879-z).
7. Chang DJ, Cho HY, Hwang S, Lee N, Choi C, Lee H, Hong KS, Oh SH, Kim HS, Shin DA, Yoon YW, Song J. Therapeutic Effect of BDNF-Overexpressing Human Neural Stem Cells (F3.BDNF) in a Contusion Model of Spinal Cord Injury in Rats. *Int J Mol Sci*. 2021 Jun 28;22(13):6970. doi: [10.3390/ijms22136970](https://doi.org/10.3390/ijms22136970).
8. Starke L, Millward JM, Prinz C, Sherazi F, Waiczies H, Lippert C, Nazaré M, Paul F, Niendorf T, Waiczies S. First in vivo fluorine-19 magnetic resonance imaging of the multiple sclerosis drug siponimod. *Theranostics* 2023; 13(4):1217-1234. doi:10.7150/thno.77041. <https://www.thno.org/v13p1217.htm>
9. Fröhlich D, Kalotay E, von Jonquieres G, Bongers A, Lee B, Suchowerska AK, Housley GD, Klugmann M. Dual-function AAV gene therapy reverses late-stage Canavan disease pathology in mice. *Front Mol Neurosci*. 2022 Dec 8;15:1061257. doi: [10.3389/fnmol.2022.1061257](https://doi.org/10.3389/fnmol.2022.1061257).

List of abbreviations

AKO = aspartoacylase-deficient lacZ-knock-in; AQP1 = aquaporin 1; ASPA = aspartoacylase; CEST = chemical exchange saturation transfer; CNS = central nervous system; EAE = experimental autoimmune encephalomyelitis; FAP = fibroblast activation protein; F3.BDNF = brain-derived neurotrophic factor; LRP = lysine-rich protein; M3P = microsized matrix-based magnetic particles; MRI = magnetic resonance imaging; MRS = magnetic resonance spectroscopy; NAA = N-acetyl-L-aspartate; oHSV = oncolytic herpes simplex virus; PARACEST = paramagnetic chemical exchange saturation transfer; PET = position emission tomography; RNA = ribonucleic acid; SPECT = single photon emission computed tomography; UTE = ultra-short echo-time; VCAM-1 = vascular cell adhesion molecule 1

Bruker BioSpin
info@bruker.com

Customer Support
<https://www.bruker.com/en/services/support.html>

Online information
bruker.com/

bruker.com

All Bruker *in vivo* animal work was approved by the institutional animal care and use committee (IACUC) or local authorities and conducted under valid study permit.

